Geophys. J. Int. (2005) **160,** 539–553 doi: 10.1111/j.1365-246X.2005.02230.x

Identification of the non-linear behaviour of liquefied and non-liquefied soils during the 1995 Kobe earthquake

Olga V. Pavlenko[1] and Kojiro Irikura[2]

[1] *Institute of Physics of the Earth, Russian Academy of Sciences, B. Gruzinskaya* 10, *Moscow* 123995, *Russia. E-mail: olga@synapse.ru*
[2] *Disaster Prevention Research Institute, Kyoto University, Gokasho, Uji, Kyoto* 611-0011, *Japan. E-mail: irikura@egmdpri01.dpri.kyoto-u.ac.jp*

Accepted 2004 January 5. Received 2003 September 18; in original form 2002 August 1

SUMMARY

A method based on the non-linear system identification technique is suggested for estimating the contents of the non-linear components, which are the result of quadratic, cubic and higher-order non-linearities, in the ground response during the strong motion. The method is applied to data from the near-fault zone of the 1995 Kobe earthquake, and the contents of linear and non-linear components in the ground response, changing with time during the strong motion, are estimated for Port Island (PI), SGK and TKS sites, located at 2, 6 and 15 km from the fault plane, respectively. At PI, the non-linear part of the response increased with developing liquefaction, it was as high as ∼ 40–60 per cent of the intensity of the response. At SGK and TKS sites, the non-linear components of the response did not exceed ∼40 and ∼13 per cent of the intensity of the response, respectively. Odd-order non-linear components predominated in the soil response, whereas even-order non-linear components increased and became comparable with odd-order ones in liquefied soils and in cases of high intensity of the strong motion, when the loading parts of the stress–strain relations of the upper layers gained noticeable even components. As a whole, the contents of odd-order and even-order components in the soil response are determined by the shapes of the stress–strain relations in the upper most non-linear soil layers. At the three sites, changes in spectra of earthquake signals in subsurface soil layers were substantial as a result of the high non-linearity of the soil behaviour and spectra of signals on the surface tend to take the form of $E(f) \sim f^{-k}$. The limiting spectral shape was achieved during the Kobe earthquake at PI and SGK sites. The proposed methods for processing vertical array records allow understanding of seismic wave transformations in subsurface soils and are useful for predicting the soil behaviour during future earthquakes.

Key words: non-linear behaviour of soils, non-linear system identification, strong ground motion, types of soil non-linearity.

1 INTRODUCTION

The non-linear behaviour of soils in strong ground motion explains the well-known fact that on soil sites, records of weak earthquakes qualitatively differ from records of strong ones. Quantitative characteristics of the soil non-linearity and estimates of the ground response at a given site during the strong motion of any arbitrary intensity are necessary for practical applications in seismology. However, because the soil response depends on many factors, such as the composition and thickness of the soft deposits, their saturation with water, the level of the underground water, and the magnitude and frequency content of an earthquake, the problem is rather complicated, and for a long time it remained as one of the urgent problems in seismology, inducing controversies and discussions.

During the 1960s–1970s, after the catastrophic earthquakes in Niigata and Anchorage, laboratory (Hardin & Drnevich 1972) and field (Vasil'ev *et al.* 1969) experiments aimed at studying non-linear elastic properties of soils began. In these experiments, non-linear hysteretic stress–strain relations were obtained for various types of soils. The questions arose, what corrections should be introduced into state equations of soils and fractured weathered rock to account for their elastic non-linearity? How large are these corrections for various types of soils and what is the threshold of strains, when they become significant? What is the mutual influence of the non-linearity of the medium, dispersion and absorption on seismic wavefields?

To estimate characteristics of elastic non-linearity of geological media, field experiments were performed and non-linear wave effects in seismic fields were studied, such as, interaction of seismic waves, generation of combination-frequency harmonics and the constant components of the wavefields, seismic solitary waves, inversion of the seismic wave front, etc. (Aleshin *et al.* 1981; Gushchin

& Shalashov 1981; Lund 1983; Shalashov 1984; Groshkov & Shalashov 1986; Dimitriu 1988, 1990; Groshkov *et al.* 1991, etc.). In these experiments, effective parameters of non-linearity, defined as the ratios of elastic parameters of the third and second, or the fourth and second orders (i.e. characteristics of the quadratic and cubic non-linearity), were estimated for subsurface soils. The obtained estimates, $N = 10^2 \div 10^4$ (Gushchin & Shalashov 1981; Shalashov 1984; Groshkov *et al.* 1991) were substantially higher than those for crystals and polycrystals: $N = 1 \div 10$ (Zarembo & Krasil'nikov 1966). This fact was explained by the model of the non-linear deformation of an inhomogeneous elastic–viscous medium. The model phenomenologically accounts for a large number of non-elastic viscous bonds with various relaxation times, which connect microblocks and macroblocks (Groshkov & Shalashov 1986). It was theoretically shown that, in conditions of loading or unloading of such a medium, the most soft bonds experience the largest deformations; as a consequence, effective values of parameters of non-linearity substantially increase (Groshkov & Shalashov 1986). As a result, non-linear corrections in state equations of geological materials become comparable with linear terms even at strains as small as $\sim 10^{-7}$ –10^{-4}, according to Gushchin & Shalashov (1981), $\sim 10^{-8}$, according to Zimenkov & Nazarov (1993), and $\sim 10^{-7}$, according to Van Den Abeele & Johnson (1996).

Observational validations of soil non-linearity were difficult to find in strong motion records, but the strong motion database grew quickly in the last decades and now seismologists can directly observe the presence of non-linear components in accelerograms as characteristic waveforms (Archuleta 1998). However, it is not often clear how much elastic non-linearity of soils influences seismic oscillations on the surface. If only records at the surface are available, it is difficult to distinguish the influence of topography, inhomogeneities in the crust, source directivity, etc. from the effects of soil non-linearity. The 1994 Northridge earthquake provided an illustrative example of the fact. Combined results from numerous alluvial recording sites testify that the decrease in the amplification of the main shock on sediments, compared with the amplification of aftershocks, was caused by a significant non-linearity of sediments (Field *et al.* 1997). However, another explanation, though rather difficult, with linear wave propagation models is also possible (O'Connell 1999).

Thus, observations of the strong motion *in situ* and seismic vertical arrays are necessary for understanding non-linear phenomena in subsurface soils (Kudo 1995; Bard & Pitilakis 1995). The behaviour of soils *in situ* in strong ground motion is not explored enough, and often it can not be satisfactorily described by the existing models and properly understood. This is partially a result of the fact that, in strong ground motion, soils do not only change the parameters of the propagating seismic waves, but they also change their properties. Phase transitions can occur, when soils are liquefied or saturated with gas bubbles. As known from physics, such multiphase media possess strong elastic non-linearity. These processes, occurring in soils in strong ground motion, are important for understanding the soil behaviour and the necessary experimental data can be obtained from observations *in situ*.

Networks of borehole instruments (Kik-Net, Japan; DART, Taipei basin; Southern California Earthquake Center, Los Angeles basin; Bay Bridges, San Francisco) are developing worldwide. Accumulation of experimental data on strong ground motion in various soil conditions could provide the answers to virtually all the questions that are interesting for seismologists. Where in the soil column does the response become non-linear? At what level of strain (stress) does the non-linear response occur? How is the non-linear response manifested in the observed ground motion? What properties of the soil that can be measured *in situ* are most important in affecting non-linearity? If a soil column experiences the non-linear response, does it return to a state with the same linear (or nearly linear) response? At what time period? (Archuleta & Steidl 2001).

Pavlenko & Irikura (2002b, 2003) have shown that strong motion records, provided by seismic vertical arrays, allow estimation of the non-linear hysteretic stress–strain relations in the soil layers at different depths from the surface down to the location of the deepest device. Records of the 1995 Kobe earthquake were analysed and vertical distributions of stress–strain relations in soil layers, changing with time during the strong motion, were obtained for Port Island (PI), SGK and TKS vertical array sites, located at distances of 2, 6 and 15 km from the fault plane, respectively.

The obtained numerical models of the soil behaviour at the three sites were tested by the Gaussian white noise, and the contents of linear and non-linear components in the soil response were estimated at the beginning, middle and final periods of the strong motion (Pavlenko & Irikura 2002b). Changes in spectra of the propagating signals were studied and it was found that spectra of signals on the surface tend to take the form of $E \sim f^{-n}$, as a result of mutual interactions of separate spectral components of propagating seismic signals. This conclusion is evidently important, because it means that in cases of strong non-linearity input signals of any arbitrary spectra are transformed in soil layers into signals of the same spectrum of the type $E \sim f^{-n}$, i.e. we loose information about the spectral compositions of input seismic signals. Deconvolution and other procedures aimed at reconstructing parameters of input signals based on surface records are impossible in cases of strong non-linearity. Therefore, it would be useful to have a representation, what strong non-linearity means and how high is the influence of the soil non-linearity on the ground response at various distances from the fault plane in various types of soils.

Vertical array records of the 1995 Kobe earthquake at PI, SGK and TKS sites provide all the necessary data for such a kind of analysis. This paper describes the detailed study of the soil behaviour at the three sites during the main shock of the Kobe earthquake and the detailed analysis of transformations of spectra of seismic signals in the near-fault areas. Estimates obtained in (Pavlenko & Irikura 2002b) are defined more exactly and completely.

2 METHOD AND DATA

In system analysis, the non-linear identification of a system implies determination of linear and non-linear domains of the system response and construction of such a mathematical model of a system that its seismic response coincides with the response of the real physical system (Marmarelis & Marmarelis 1978). Soil profiles can be represented as non-linear systems (because of the non-linear stress–strain relations), transforming input seismic signals into the ground response, i.e. movement on the surface. The most quick and effective method for the non-linear system identification is testing the studied system with the Gaussian white noise and calculating the Wiener kernels (Marmarelis & Marmarelis 1978). If an input is the Gaussian white noise, an output can be represented as the Wiener series (Marmarelis & Marmarelis 1978):

$$y(t) = \sum_{m=0}^{\infty} G_m[h_m(\tau_l, \cdots, \tau_m); x(t'), t' \le t], \tag{1}$$

where G_m are orthogonal functionals, if $x(t)$ is the Gaussian white noise with a zero mean, $\{h_m(\tau_1, \ldots, \tau_m)\}$ is a sequence of the Wiener kernels and $\tau_1, \ldots, \tau_m$ are time delays. The first four Wiener

functionals are:

$$G_0[h_0; x(t)] = h_0, \tag{2}$$

$$G_1[h_1; x(t)] = \int_0^\infty h_1(\tau)x(t-\tau)d\tau, \tag{3}$$

$$G_2[h_2; x(t)] = \int_0\int^\infty h_2(\tau_1, \tau_2)x(t-\tau_1)x(t-\tau_2)\,d\tau_1\,d\tau_2 - P\int_0^\infty h_2(\tau_1, \tau_1)\,d\tau_1, \tag{4}$$

$$G_3[h_3; x(t)] = \int\int_0^\infty\int h_3(\tau_1, \tau_2, \tau_3)x(t-\tau_1) \times x(t-\tau_2)x(t-\tau_3)\,d\tau_1\,d\tau_2\,d\tau_3 - 3P\int_0^\infty\int h_3(\tau_1, \tau_2, \tau_2)x(t-\tau_1)\,d\tau_1\,d\tau_2, \tag{5}$$

where τ is time delay and P is the intensity of the Gaussian white noise not depending on frequency.

Orthogonality of terms in the Wiener series provides substantial advantages in the non-linear system analysis, because the Wiener kernels can be easily calculated by the method of the cross-correlation functions and a limited number of terms in the Wiener series represent the best approximation for a real system from the viewpoint of the minimal mean square error (Marmarelis & Marmarelis 1978). By analogy with an ordinary impulse characteristic $h(t)$, kernel series $\{h_m\}$ can be treated as a generalized, composed impulse characteristic of a non-linear system. The first-order kernel determines the linear part of the system response, whereas higher-order kernels describe the quadratic, cubic and higher-order non-linear corrections. The non-linear corrections express interactions between the values of the input signal in the past with respect to their influence on the response at present. Analysing the non-linear components in the output, we can make a judgement about the types and quantitative characteristics of the system non-linearity: if the second Wiener functional G_2 provides the largest contribution to the system response, the system possesses mostly quadratic non-linearity; if the third functional G_3 contributes more, the system is cubic non-linear, etc. (Marmarelis & Marmarelis 1978). Knowledge of stress–strain relations in soil layers in strong ground motion allows calculation of the propagation of testing signals in the studied soil profiles and the non-linear identification of the soil behaviour (Pavlenko 2001).

We applied these methods to perform the non-linear identification of the behaviour of soils at PI, SGK and TKS vertical array sites during the 1995 Kobe earthquake. Fig. 1 shows the locations of these sites, the major principal axes, epicentres of the main shock and aftershocks and the soil profiles. The procedure of estimation of stress–strain relations in soil layers is described in detail in (Pavlenko & Irikura 2003). The soil profiles were divided into groups of layers, according to their composition and saturation with water. For these groups, physically justified types of stress–strain relations were assumed. Sets of parametric stress–strain curves were generated and item-by-item examination was applied to find groups of curves showing the best-fitting approximation to the observed data. To account for temporal changes in the soil behaviour, records were divided into intervals of 1.5-s duration. Within each interval, the stress–strain relations were assumed to be stationary and to vary for different intervals. Calculations were performed successively, interval by interval.

The observed and simulated acceleration time histories of the main shock (horizontal components) and 10 successive time intervals used in our calculations are shown in Fig. 2. Fig. 3 illustrates estimated hysteretic non-linear stress–strain relations, averaged within the groups of the upper layers at PI, SGK and TKS sites. The whole set of stress–strain relations, obtained for all the depths, from the surface down to the location of the deepest device, is given in (Pavlenko & Irikura 2003). Because in our calculations stress–strain relations are represented in their normalized form as suggested by Joyner & Chen (1975), so that the same relations describe the behaviour of different layers within a group, averaging of stress–strain relations within a group means finding average working intervals of the normalized stress–strain relations within the group.

Thus, numerical models of the soil behaviour during the 1995 Kobe earthquake were constructed for PI, SGK and TKS sites. Reliability of the obtained representations at the three sites is verified by the following.

(i) A good agreement between the observed and simulated records and similarity of the stress–strain relations obtained for two horizontal components (Figs 2 and 3).

(ii) Physical correctness of the description of the process: progressive liquefaction in the upper layers at PI, reduction and recovery of the shear moduli in the upper layers at SGK and TKS, and stable behaviour in deeper parts at the three sites.

(iii) An agreement between our estimates and conclusions of other authors (Kawase *et al.* 1995; Sato *et al.* 1996; Kazama *et al.* 1998).

The obtained numerical models were used for the non-linear identification of the soil behaviour during the 1995 Kobe earthquake at the three sites, i.e. for estimation of the contents of non-linear components in the soil response at these sites. In the non-linear identification, before calculating Wiener kernels and functionals, the studied non-linear system is usually tested by monochromatic signals, in order to reveal the types and roughly estimate some quantitative characteristics of the system non-linearity.

Testing signals used in our calculations, such as monochromatic signals and the Gaussian white noise, were approximations to the input seismic signals during the Kobe earthquake. As seen from formulae (2)–(5), estimates of the Wiener kernels depend on the intensity of the testing Gaussian white noise. To obtain reliable estimates of the Wiener kernels, we tried to attain conditions of propagation of testing signals close to real seismic waves during the earthquake. We chose the intensity of testing signals so that the working intervals of stress–strain relations during the propagation of these signals in the soil layers were close to those ones during the propagation of signals from the earthquake. However, in a layered medium, propagation features of seismic signals with different spectral compositions are different and, in general, it is not possible to choose such intensity of testing signals that the working intervals of stress–strain relations during the propagation of testing signals coincide with those ones during the earthquake. Therefore, we chose the controlling parameters, such as mean-square stresses, mean-square strains and mean-square slopes of the stress–strain curves, within the groups of layers, and in choosing the intensities of testing signals, we tried to adjust these parameters for the groups of layers. Two groups of layers were considered for SGK and TKS sites and five groups of layers for PI, as shown in Fig. 1.

In our previous study (Pavlenko & Irikura 2002b), only one parameter was used to adjust the intensity of testing Gaussian white noise signals, such as an average slope of the stress–strain curves in the groups of the upper layers. However, numerical examples show that more exact estimates of Wiener kernels are obtained if we use more parameters. In addition, we substantially increased the duration

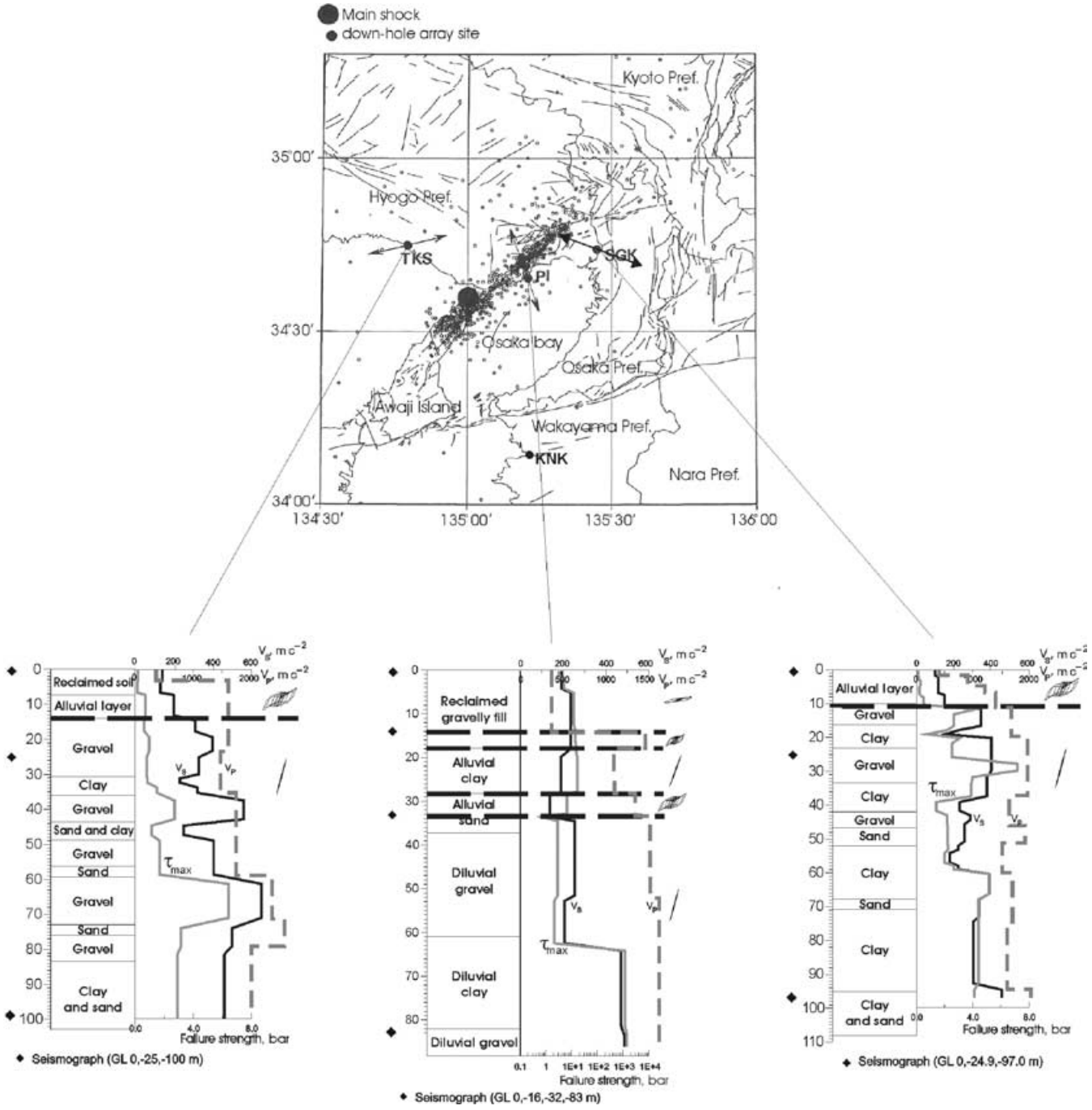

Figure 1. Locations of vertical array sites Port Island (PI), SGK and TKS around the Osaka bay, the major principal axes, the epicentres of the main shock and aftershocks (derived from Sato *et al.* 1996) and the ground profiles and characteristic types of stress–strain relations.

of testing Gaussian white noise signals compared with our previous study (Pavlenko & Irikura 2002b), because this also leads to more accurate and reliable estimates of Wiener kernels and functionals (Marmarelis & Marmarelis 1978).

3 RESULTS AND DISCUSSION

Fig. 4 presents the results of testing the obtained models of the soil behaviour (East-West components) during the 1995 Kobe earthquake at the three sites with monochromatic signals. Spectra of input monochromatic signals are shown in lower rows at each site and above them are spectra of simulated signals at depths of locations of the recording devices for 10 successive time intervals. As seen from the figure, signals, propagating up to the surface, acquire higher harmonics of the main frequencies. The higher harmonics of the main frequencies, which are generated during the propagation of the monochromatic signals in the soil layers, indicate the types of elastic non-linearity of the soil profiles. A large number of the higher harmonics at PI and SGK sites testifies to a strong non-linearity of the soil behaviour at these sites. Whereas at TKS site, few higher harmonics are generated indicating a weaker non-linearity of the soil behaviour at TKS site. Generation of the third, fifth, seventh and other

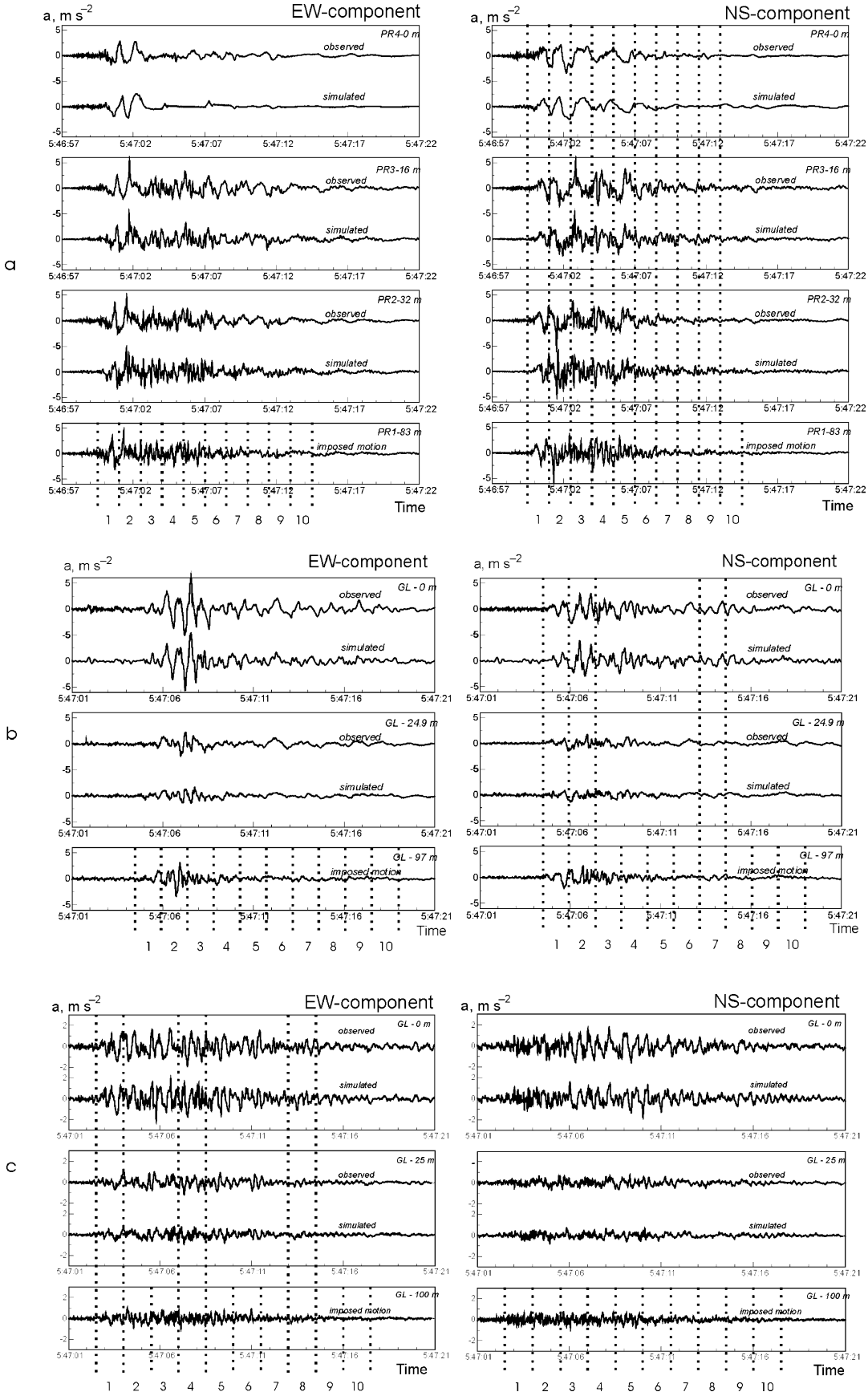

Figure 2. Acceleration time histories of the main shock of the 1995 Kobe earthquake, observed and simulated, at PI (a), SGK (b) and TKS (c) sites. Dash lines indicated selected intervals, for which the results of the non-linear identification are shown in Figs 5(a)–(c).

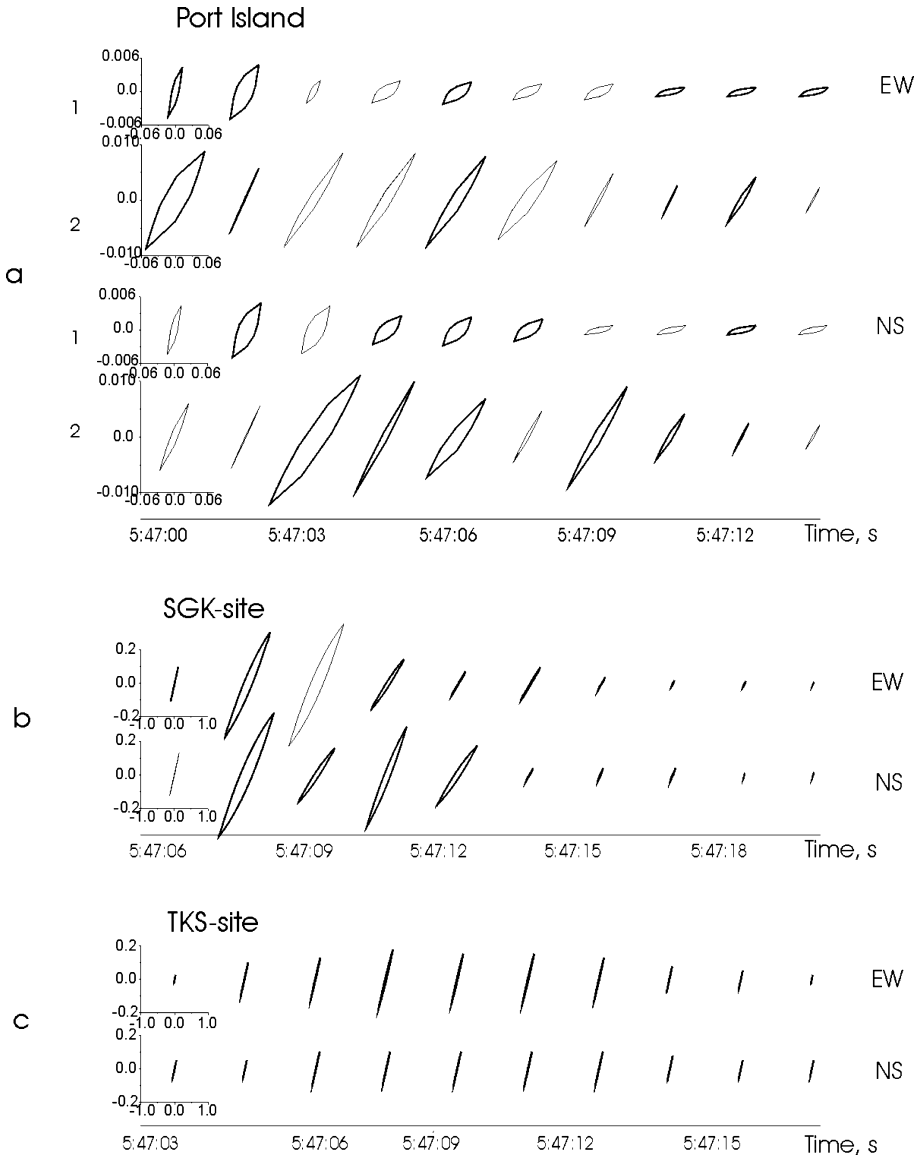

Figure 3. Estimated stress–strain relations in the soil layers during the 1995 Kobe earthquake, averaged within the groups of layers at (a) PI (1: 0–13 m and 2: 13–17.5 m), (b) SGK (0–11 m) and (c) TKS (0–14 m), for 10 successive time intervals. Scales in relative units are the same for all time intervals. Stress and strain are scaled in the manner described by Joyner & Chen (1975): stress is normalized by multiplying by $1/\tau_{\max}$ and strain is normalized by multiplying by $G_{\max}/\tau_{\max}$.

odd-order harmonics testifies to odd-order non-linearities of the soil behaviour. Even-order higher harmonics, such as the second, fourth, etc., are generated only in liquefied soils at PI and at SGK site during the second and third time intervals of the strong motion.

Because non-linear hysteretic stress–strain relations determine transformations of input seismic signals into the ground response, generation of higher harmonics obviously depends on the shapes of the stress–strain curves. Loading and unloading parts of the hysteretic stress–strain curves can be represented as sums of even and odd functions (as known, any function defined within the area $[-x; x]$ can be represented as a sum of an even function $0.5^*[f(x) + f(-x)]$ and an odd function $0.5^*[f(x) - f(-x)]$ Korn & Korn 1968) and the odd components of the loading parts of the stress–strain curves obtained for the three sites are usually larger than the even components, except the latter intervals in the upper 13 m at PI, where the stress–strain curves are very sloping (Fig. 3), and the even and odd components are approximately equal. Even-order higher harmonics are generated in the latter intervals at PI and at SGK site, where the corresponding stress–strain curves gained noticeable even components, and we can conclude that odd-order non-linearities are typical for soils, whereas even-order non-linearities appear only in cases when the loading (and unloading) parts of stress–strain relations represent functions with noticeable even components.

We should emphasize the difference between the described effects of higher harmonic generation and the resonant amplification of seismic signals in the upper soft soil layers. As known, resonant spectral peaks are usually wide and fuzzy, in contrast to spectra shown in Fig. 4. Here, we consider non-linear distortions of the propagating monochromatic signals, which are caused by the non-linearity of the hysteretic stress–strain relations describing the behaviour of the soil layers. For any frequencies of input signals, we will obtain the same patterns of higher harmonics generation similar to those shown in Fig. 4, which do not depend on the boundary conditions of the models.

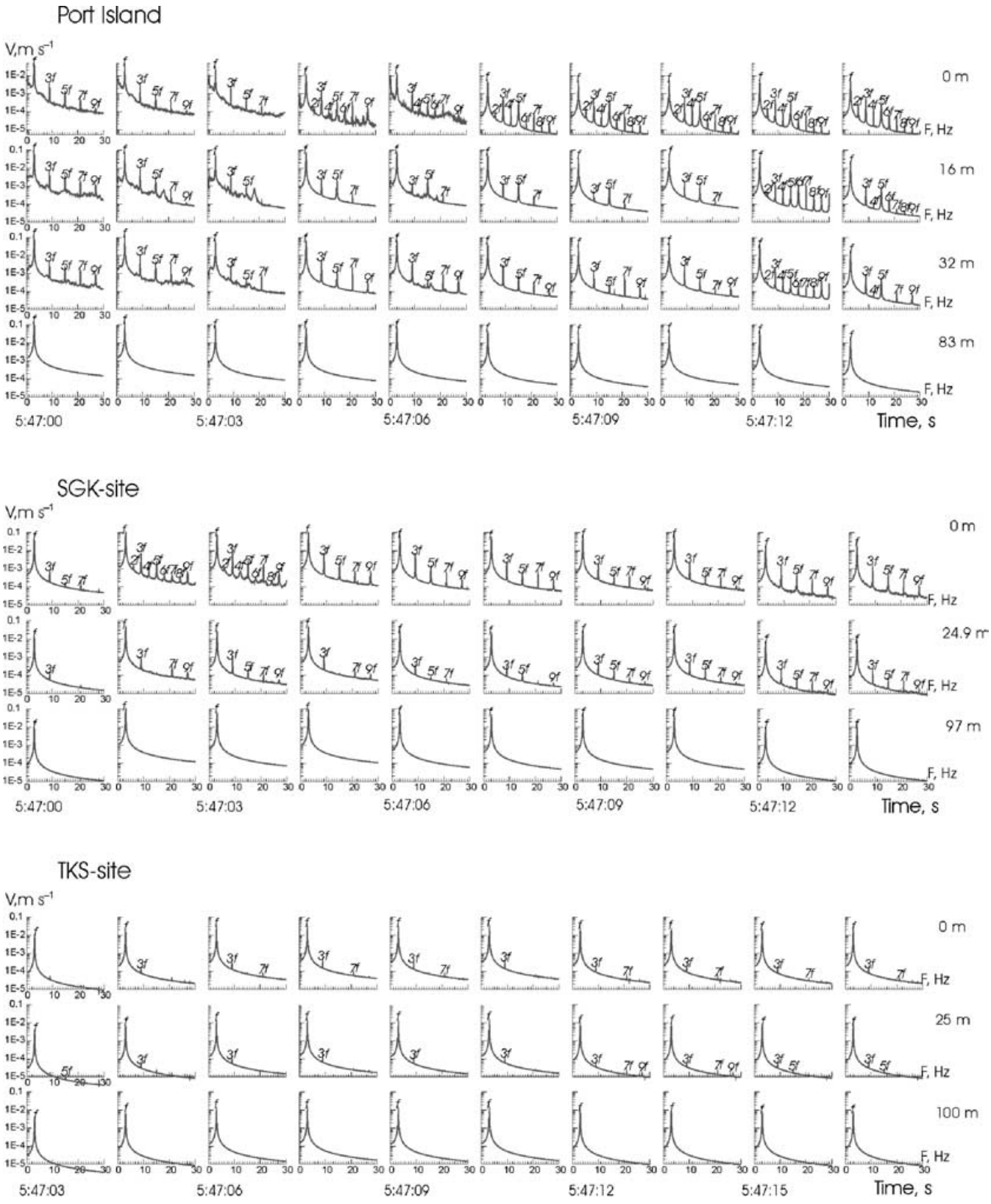

Figure 4. Velocity spectra of testing monochromatic signals, propagating in soil layers, at depths of locations of the recording devices at PI (0, 16, 32 and 83 m), SGK (0, 24.9 and 97 m) and TKS (0, 25 and 100 m), for 10 successive time intervals.

The results of testing our models by the Gaussian white noise in 10 successive time intervals are shown in Figs 5(a)–(c) and 6, and in Tables 1 and 2. Functionals of the Wiener series were calculated by the method of cross-correlation functions (Marmarelis & Marmarelis 1978), and linear, non-linear quadratic, non-linear cubic components and constant components of the ground response were estimated according to formulae (2)–(5). Estimates of the zero-, first-, second- and third-order kernels are based on input and output signals of 500 000 points of duration (more than 40 min). These kernels were used to calculate the responses of the linear models and the non-linear corrections accounting for quadratic and cubic non-linearities.

Figs 5(a)–(c) and Table 1 show the non-linear components of the soil responses at PI (Fig. 5a), SGK (Fig. 5b) and TKS (Fig. 5c) sites, and the non-linear quadratic and cubic components in percentages of the whole intensity of the responses. At PI, liquefaction occurred in the upper layers and five time intervals are shown in Fig. 5(a), corresponding to different stages of liquefaction. Figs 5(b) and (c) represent examples of the non-linear identification of the soil behaviour at the beginning, middle and final periods of the strong motion at SGK and TKS sites. The results of the non-linear identification of the soil behaviour in 10 successive time intervals during the 1995 Kobe earthquake at the three sites are given in Table 1.

A noticeable difference in the shapes of input and output signals at PI (Fig. 5a) indicates a high non-linearity of the soil behaviour of the upper layers, which increases with developing liquefaction. A substantial non-linear component appears in the response of soils at PI even during the first seconds of the strong motion, which increases from ∼40 to ∼60 per cent with developing liquefaction (Fig. 5a, Table 1). At the beginning of the strong motion, the non-linear cubic component of the response substantially exceeds the non-linear quadratic one. As liquefaction developed at PI, the non-linear quadratic component of the response increased, whereas the non-linear cubic component slightly decreased, so that their parts in the soil response became approximately equal in liquefied soils. At the same time, the residual part of the soil response, which is partially the result of higher-order non-linearities, noticeably increased with developing liquefaction, indicating an increase in the higher-order (the fourth-, fifth-, sixth-order, etc.) non-linearities of the soil response at PI. Estimates presented in Table 1 reveal these tendencies, except the last time interval, where the non-linear components of the soil response are weaker because of the decrease in the intensity of the strong motion.

The residual parts of the response, remaining after subtraction of linear, non-linear quadratic and non-linear cubic components from the responses, characterize the parts of the higher-order non-linearities, as well as inaccuracies of the estimates (Marmarelis & Marmarelis 1978). The inaccuracies are caused by the finite duration and the boundedness of the spectral band of the Gaussian noise, by truncation of tails of the normal distribution of noise amplitudes and by inaccuracies in calculations. The detailed error analysis and correction methods are given in (Marmarelis & Marmarelis 1978). To evaluate the level of inaccuracies in the obtained estimates, we performed numerical simulations with linear models, where linear stress–strain relationships, similar to Hooke's law, were used instead of the non-linear hysteretic ones. We found that for the selected duration of testing Gaussian white noise signals (500 000 points) estimated non-linear components of the responses of linear models do not exceed 0.8–1 per cent of the intensity of the response. We took these values as a rough estimate of the accuracy of our calculations of the Wiener functionals in the non-linear identification. However, inaccuracies in estimates of the contents of the non-linear components in the soil response during the 1995 Kobe earthquake at PI, SGK and TKS sites are evidently higher, up to some per cent, because they account for deviations of the constructed numerical models of the soil behaviour during the 1995 Kobe earthquake at these sites from the real soil behaviour.

At SGK site, changes in the behaviour of the upper layers during the earthquake were also high and the non-linear part of the response reached ∼39 per cent, whereas at TKS site it did not exceed ∼13 per cent. As seen from Table 1 and Figs 5(b) and (c), the parts of non-linear components in the soil response at SGK and TKS sites change in accord with the intensity of the strong motion: they are small at the beginning and at the end of the strong motion, but they grow up and reach their maxima in the middle of the strong motion at moments of its highest intensity. The quadratic, cubic and higher-order non-linear components of the response show similar trends and the non-linear cubic components are substantially higher than the non-linear ratic ones. On the whole, the non-linear components of the response are noticeably higher at SGK than at TKS site (Table 1).

Zero-order kernels h_0 represent quasi-static deformations of the surface, that is, non-zero values of h_0 indicate slow shifting of the surface layers to one or the other side in their oscillations. This effect can be interpreted as a result of accumulation of residual shift deformations on the surface (Zvolinskii 1982). The asymmetry of oscillations is connected with even-order non-linearities (Marmarelis & Marmarelis 1978). Figs 5(a)–(c) show the values of the quasi-static deformations, obtained in our numerical simulations. Higher values of the quasi-static deformations at PI site and in the second time interval at SGK site compared with similar values for TKS site indicate higher contents of the even-order non-linearities in the soil response at PI and SGK sites. At PI, the quasi-static deformations increase with developing liquefaction, indicating an increase in the even-order non-linearities.

Below in Figs 5(a)–(c), values of the first-order Wiener kernel $h_1(\tau)$, the diagonal values of Wiener kernels $h_2(\tau_1, \tau_2)$ and $h_3(\tau_1, \tau_2, \tau_3)$, and averaged within the upper layers stress–strain relations, which are due to the propagation of the Gaussian white noise in the soil profiles at PI, SGK and TKS sites, are presented. To discuss the meaning of the Wiener kernels, let us represent the loading (or unloading) parts of the stress–strain relations as the power series

$$\sigma(\varepsilon) = a_1\varepsilon + a_2\varepsilon^2 + a_3\varepsilon^3 + a_4\varepsilon^4 + a_5\varepsilon^5 + \ldots, \quad (6)$$

where σ is stress, ε is strain and a_1, a_2, a_3, a_4, a_5 are constant coefficients. The first term in the series $a_1\varepsilon$ describes the linear dependence (the Hooke's law); the others are non-linear corrections. In this representation, the first-order kernel $h_1(\tau)$ is related to the linear term, so that the maximum of the function $h_1(\tau)$, corresponding to the time of seismic wave propagation from the depth of location of the deepest device to the surface, estimates coefficient a_1, whereas $h_2(\tau_1, \tau_2)$ and $h_3(\tau_1, \tau_2, \tau_3)$ are related to the quadratic and cubic non-linear corrections, and maxima or minima of $h_2(\tau, \tau)$ and $h_3(\tau, \tau, \tau)$ [achieved at the same time delays as maxima of $h_1(\tau)$] evaluate coefficients a_2 and a_3, respectively.

We can see from Figs 5(a)–(c) that the first-order kernels $h_1(\tau)$ and the diagonal values of the second- and third-order kernels $h_2(\tau_1, \tau_2)$ and $h_3(\tau_1, \tau_2, \tau_3)$ change with time during the strong motion, and the diagonal values of $h_3(\tau_1, \tau_2, \tau_3)$ are usually substantially higher than the diagonal values of $h_2(\tau_1, \tau_2)$ and $h_1(\tau)$, especially at the beginning of the strong motion in the domain of small strains and large values of a_1. The obtained estimates indicate a high variability of functions $h_2(\tau_1, \tau_2)$ and $h_3(\tau_1, \tau_2, \tau_3)$, especially $h_3(\tau_1, \tau_2, \tau_3)$, during the strong motion and a wide range of their variations.

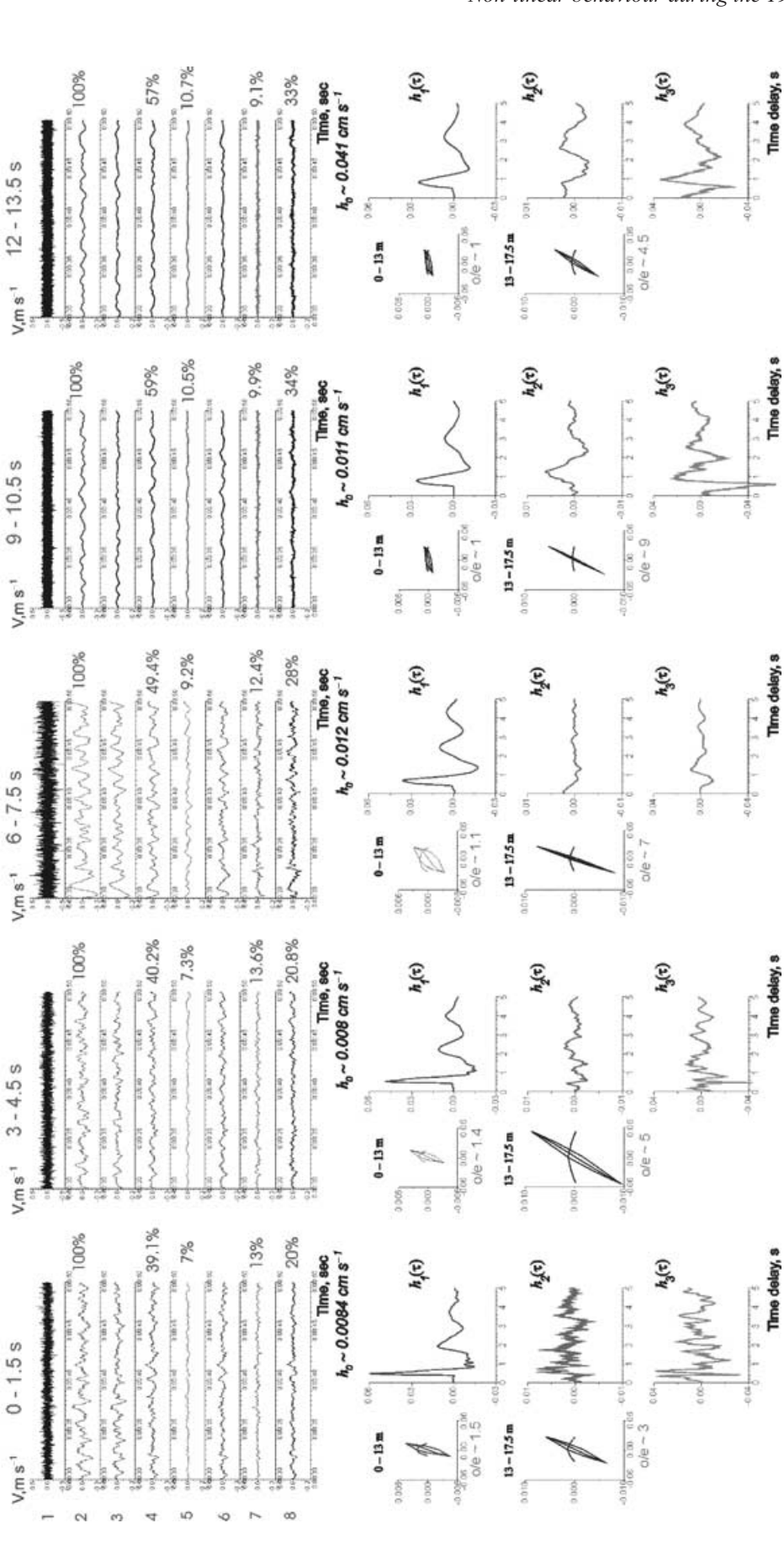

Figure 5. Testing of soil layers with the Gaussian white noise at sites (a) PI (NS component, intervals 1, 3, 5, 7 and 9) for five different stages of liquefaction, (b) SGK (NS component, intervals 1, 2 and 7) and (c) TKS (EW component, intervals 1, 4 and 8). 1 is the input signal, 2 is the output, 3 is the response predicted by a linear model, 4 is the difference between the response of the system and the response predicted by a linear model, 5 is the non-linear correction as a result of quadratic non-linearity predicted by kernel $\{h_2\}$, 6 is the difference between the response of the system and the response predicted by model $\{h_0, h_1, h_2\}$, 7 is the non-linear correction as a result of cubic non-linearity predicted by kernel $\{h_3\}$, and 8 is the difference between the response of the system and the response predicted by model $\{h_0, h_1, h_2, h_3\}$. Below are shown corresponding average stress–strain relations for groups of layers, represented as even and odd functions, and diagonal value of kernels of the first, second and third orders. Values o/e are the ratios of the amplitudes of the even and odd functions. Zero-order kernels h_0 increase with developing liquefaction.

b

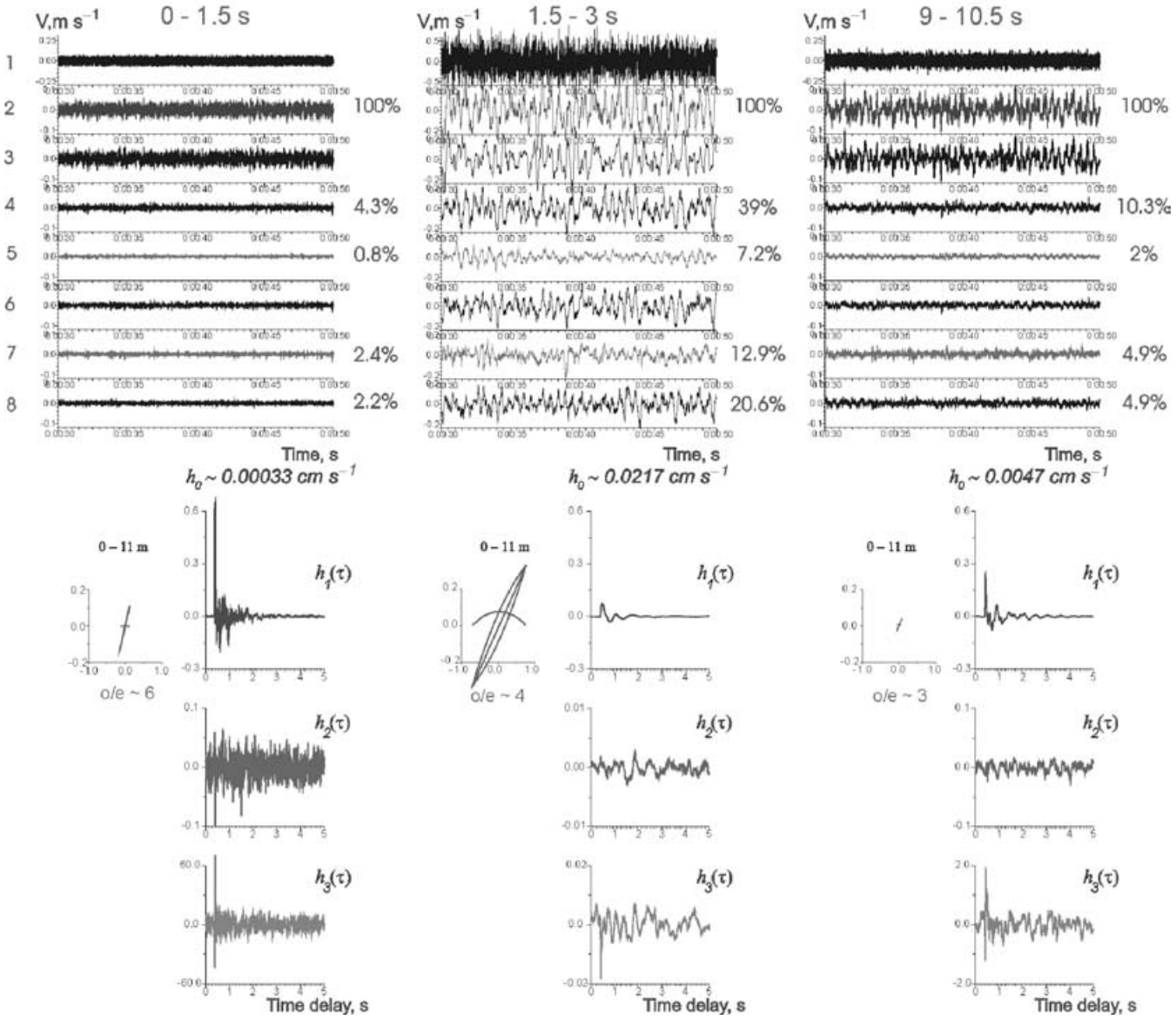

Figure 5. (*Continued.*)

As Figs 5(a)–(c) show, extreme values of $h_3(\tau_1, \tau_2, \tau_3)$ can be tens or hundreds of times higher than $h_1(\tau)$. Thus, our results explain high values of effective parameters of elastic non-linearity in subsurface soils of $\sim 10^2 \div 10^4$, obtained in field experiments (Gushchin & Shalashov 1981; Shalashov 1984; Groshkov *et al.* 1991), as well as their large variations. Because seismology deals with a wide range of strain levels and, moreover, soils can change their properties during the strong motion, large variations of the effective parameters of non-linearity are easy to understand. According to our estimates, the range of strains during the 1995 Kobe earthquake at the three sites was approximately 10^{-5}–10^{-3}.

Loading and unloading parts of the hysteretic stress–strain curves can be represented as sums of even and odd functions, and our results confirm that the relationships between the even and odd components of the stress–strain curves define the relationships between even-order and odd-order non-linear components of the soil response. Figs 5(a)–(c) show even and odd components of the loading parts of the stress–strain curves together with the stress–strain curves: convex-up arcs crossing the hysteretic loops represent the even components and diagonal lines inside the loops show the odd components. Ratios of the amplitudes of the odd to the even components are designated as o/e and also shown in the figure.

As liquefaction developed at PI, the stress–strain relations in the upper layers became more and more sloping, the even components of the loading parts of the stress–strain curves increased and the even-order non-linear components in the soil response increased (Fig. 5a). Loading parts of the stress–strain relations describing the behaviour of the upper soil layers at SGK site also gained substantial even components, when the intensity of the strong motion increased to its highest values; as a result, noticeable even-order non-linear

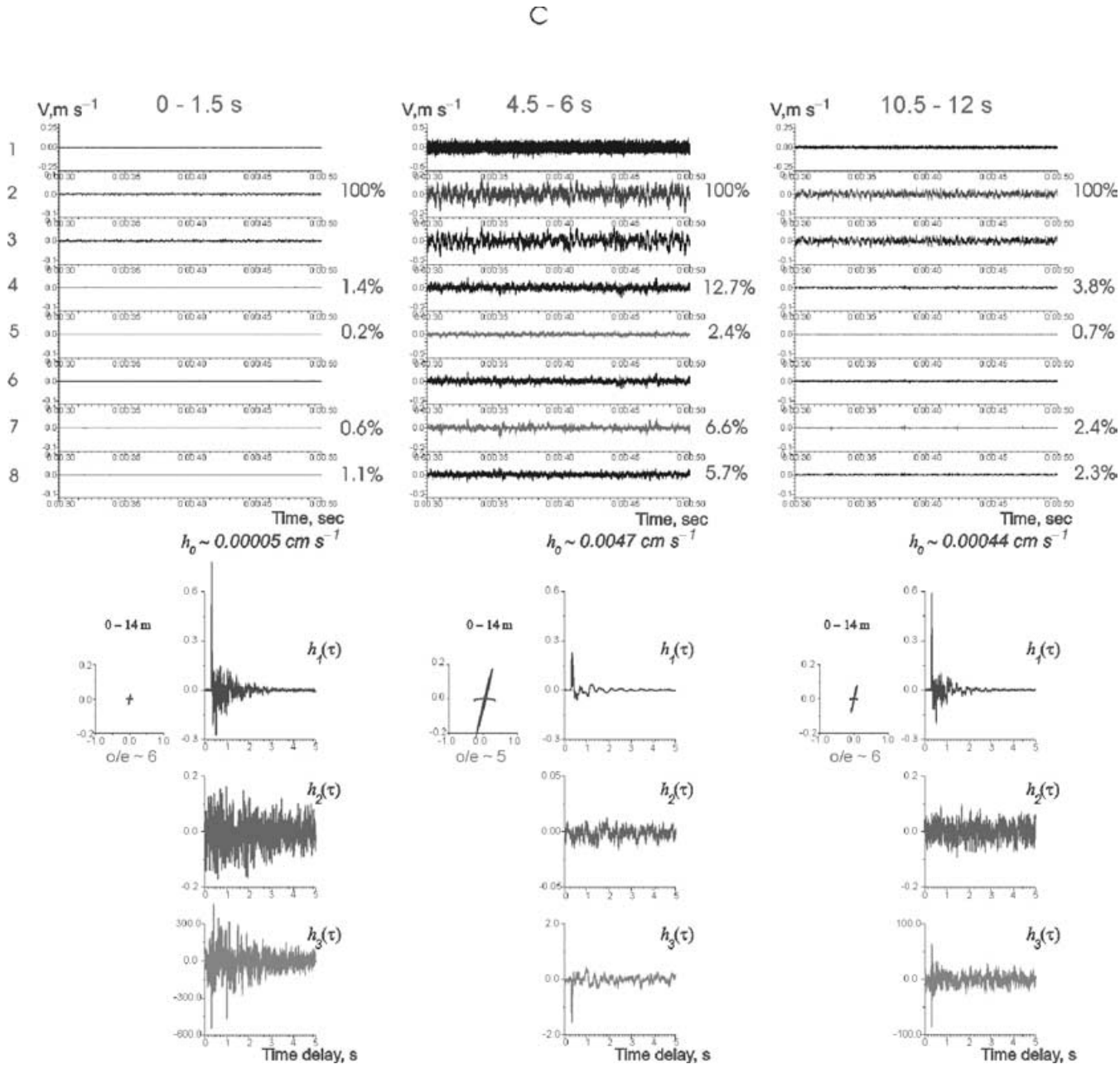

Figure 5. (*Continue.*)

components appeared in the soil response at SGK (Fig. 5b). At TKS site, the intensity of the strong motion was not so high, the loading parts of the stress–strain relations describing the soil behaviour represent predominantly odd functions and even-order non-linear components in the soil response were weak (Fig. 5c).

At the three sites, temporal changes in the Wiener kernels during the strong motion are significant (Figs 5a–c). At PI, maxima of the first-order Wiener kernels $h_1(\tau)$ decrease and shift to larger time delays, which is a result of the increased sloping of the stress–strain relations. Amplification of seismic waves decrease and shear moduli in the upper layers decrease with developing liquefaction, whereas the traveltimes of seismic waves increase. At the same time, the first-order kernels become smoother and wider, which testifies to the rising predominance of low-frequency oscillations on the surface, and the second-order kernels $h_2(\tau_1, \tau_2)$ grow and smooth with developing liquefaction. At SGK and TKS sites, changes in the Wiener kernels are also substantial, and we can note that an increase in the intensity of the strong motion leads to smoothing of the Wiener kernels and decreasing their amplitudes.

Fig. 6 demonstrates spectra of testing Gaussian white noise signals, obtained in our numerical simulations, at depths of locations of the recording devices at the three sites in 10 successive time intervals. These spectra show an important tendency of spectral transformations in the soil layers, such as, spectra of signals on the surface tend to take the form of $E(f) \sim f^{-k}$ (Fig. 6). Shapes of spectra at intermediate depths (16 and 32 m at PI; 24.9 m at SGK and 25 m at TKS) testify to the resonant amplification of some spectral components in the inner layers. At the same time, interactions of the spectral components take place together with their resonant amplification and lead to generation of combination-frequency

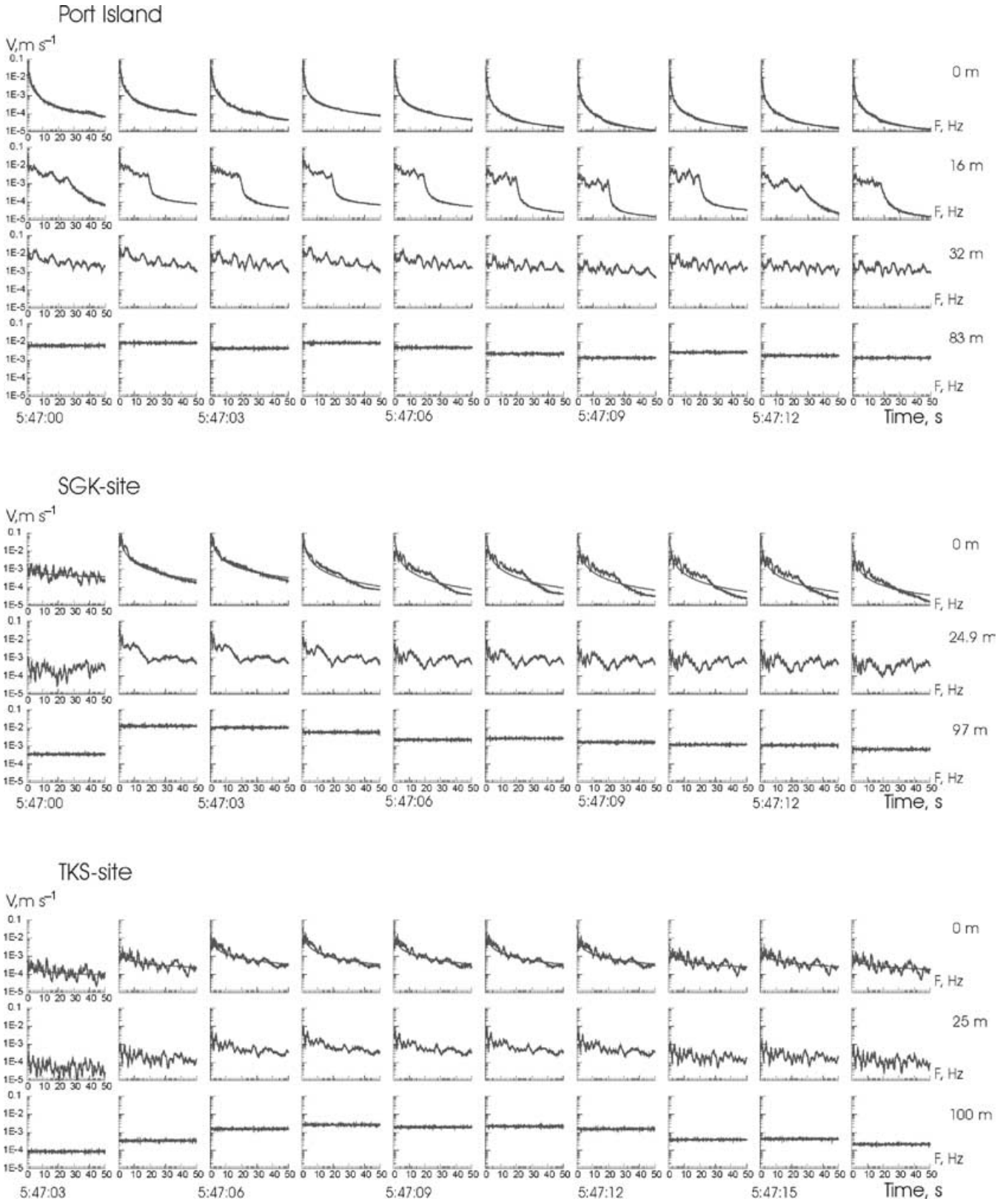

Figure 6. Velocity spectra of the testing Gaussian white noise, propagating in soil layers, at depths of locations of the recording devices at PI (0, 16, 32 and 83 m), SGK (0, 24.9 and 97 m) and TKS (0, 25 and 100 m), for 10 successive time intervals.

Table 1. Non-linear components of the soil response estimated in the numerical simulation with the Gaussian white noise.

		Number of time interval	1	2	3	4	5	6	7	8	9	10
Port	EW	**nl**	**41.9**	**49.7**	**37.7**	**54.5**	**46**	**53.1**	**53**	**54.2**	**59.3**	**48.3**
Island		nl-2	8.7	9.4	7.3	10.6	8.7	10.1	10.2	10.5	11.8	8.6
		nl-3	14.3	13.2	11.5	12.9	10.6	9.2	9.0	9.1	9.9	8.7
		res	21.3	27.3	20.2	30.5	28.6	31.3	30.6	31.3	33.3	28.8
		nl	**39.1**	**51.2**	**40.2**	**39.3**	**49.4**	**44.8**	**59**	**53.2**	**56.9**	**47.2**
		nl-2	7.2	9.5	7.3	7.3	9.2	8.3	10.5	9.3	10.7	9.1
	NS	nl-3	12.9	14	13.6	13.4	12.4	13.2	9.9	9.5	9.1	9
		res	20.3	27.5	20.8	20.3	28.1	23.8	34.9	31.5	33.4	27.3
SGK	EW	**nl**	**4.3**	**39.1**	**35.2**	**28.8**	**33.6**	**11.1**	**10.3**	**9.7**	**8.9**	**8.9**
		nl-2	0.8	7.3	6.7	5.3	6.4	2.1	2	1.8	1.7	1.7
		nl-3	2.3	12.9	11.9	11.2	11.4	4.9	4.9	4.4	3.8	3.7
		res	2.2	20.6	17.7	14.9	17.7	5.4	4.9	4.7	4.6	4.5
		nl	**3.4**	**27.4**	**37.5**	**33.9**	**14.8**	**22.5**	**11.3**	**8.2**	**7.6**	**6.2**
		nl-2	0.6	5.1	6.6	6.4	2.8	4.4	2.1	1.6	1.4	1.2
	NS	nl-3	1.7	9.2	18.8	12.2	6.8	8.4	5	3.7	3.6	2.5
		res	1.8	13.8	26.4	17.3	7.4	11.2	5.5	4.1	4	3.1
TKS	EW	**nl**	**1.8**	**4.3**	**6.2**	**7.3**	**6.1**	**7.5**	**5.7**	**4.6**	**2.9**	**3.2**
		nl-2	0.3	0.8	1.2	1.4	1.2	1.4	1.1	0.9	0.5	0.6
		nl-3	0.8	2.2	3	3.7	2.9	4.4	3	2.3	1.3	1.9
		res	1.2	2.3	2.8	3.3	2.8	3.7	2.8	2.4	1.6	2
	NS	**nl**	**1.4**	**3.5**	**9.1**	**12.7**	**10.5**	**11.1**	**9.1**	**3.8**	**4.1**	**2.5**
		nl-2	0.3	0.7	1.7	2.4	2	2.1	1.7	0.7	0.8	0.5
		nl-3	0.6	2	5.2	6.6	5.3	5.8	5.1	2.3	2	1.1
		res	1.1	2.2	4.4	5.7	4.6	5.1	4.5	2.4	2	1.5

nl is the non-linear part of the response, which represents the deviation of the response of a real system from the response of the linear model constructed by the zero- and first-order kernels $\{h_0, h_1\}$;
nl-2 is the non-linear correction as a result of quadratic non-linearity predicted by kernel $\{h_2\}$;
nl-3 is the non-linear correction as a result of cubic non-linearity predicted by kernel $\{h_3\}$;
res- the deviation of the system response from the response of the non-linear model predicted by kernels $\{h_0, h_1, h_2, h_3\}$.

Table 2. Coefficient k estimated in the numerical simulation with the Gaussian white noise in 10 successive time intervals and from the surface velosigramms of the 1995 Kobe earthquake (the last column).

	Number of time interval	1	2	3	4	5	6	7	8	9	10	EQ
Port	EW	**−1.33**	**−1.3**	**−1.35**	**−1.18**	**−1.24**	**−1.23**	**−1.31**	**−1.13**	**−1.28**	**−1.32**	**−1.21**
Island	NS	**−1.31**	**−1.31**	**−1.35**	**−1.37**	**−1.28**	**−1.43**	**−1.25**	**−1.26**	**−1.22**	**−1.44**	**−1.39**
SGR	EW	−0.31	**−1.28**	−1.51	−1.1	−1.43	−1.46	−1.3	−1.28	−1.08	−1.08	−1.46
	NS	−0.25	**−1.41**	**−1.26**	−1.51	−1.48	−1.48	−1.45	−1.43	−1.42	−1.34	−1.39
TKS	EW	−0.32	−0.51	−0.62	−0.69	−0.63	−0.69	−0.6	−0.52	−0.4	−0.43	−1.45
	NS	−0.29	−0.45	−0.79	−0.95	−0.86	−0.89	−0.79	−0.47	−0.49	−0.38	−1.56

harmonics in the low and high frequency ranges, amplitudes of combination harmonics being related to their frequencies (Zarembo & Krasil'nikov 1966). As a result, the energy is redistributed over the spectral band so that low-frequency components increase, sharp spectral peaks disappear and the resulting spectrum of the output tends to take the limiting smooth form of $E(f) \sim f^{-k}$ (Fig. 6).

Table 2 represents estimates of coefficient k obtained in our numerical simulation with the Gaussian white noise in 10 successive time intervals and coefficient k estimated from the surface velosigramms of the 1995 Kobe earthquake. As is seen from the table, at PI, coefficient k does not change much with developing liquefaction and varies within the limits of ∼1.13 to ∼1.44, whereas at SGK and TKS, variations of coefficient k are substantial. Note that in cases when spectra of signals on the surface can be accurately approximated by expression $E \sim f^{-k}$, k values are close to 1.3 ÷ 1.4 (Fig. 6, Table 2). These cases are marked in bold in Table 2. Non-linear distortions of the propagating signals were high at PI and all the spectra of signals on the surface took the smooth form of $E \sim f^{-k}$ (Fig. 6). At SGK and TKS sites, non-linearity was not so strong and spectra of signals on the surface approach their limiting form only at SGK in the intervals of the highest intensity of the strong motion, and in these cases coefficients k take values similar to those at PI, i.e. 1.26–1.41. At TKS site, spectra of signals on the surface can not be accurately approximated by expression $E \sim f^{-k}$ and coefficients k vary during the strong motion, increasing in its middle period.

Values of coefficient k estimated from the surface velosigramms of the 1995 Kobe earthquake are shown in the last column in Table 2. These values are close to those obtained in the numerical simulation with the Gaussian white noise, especially for PI. Velocity spectra of

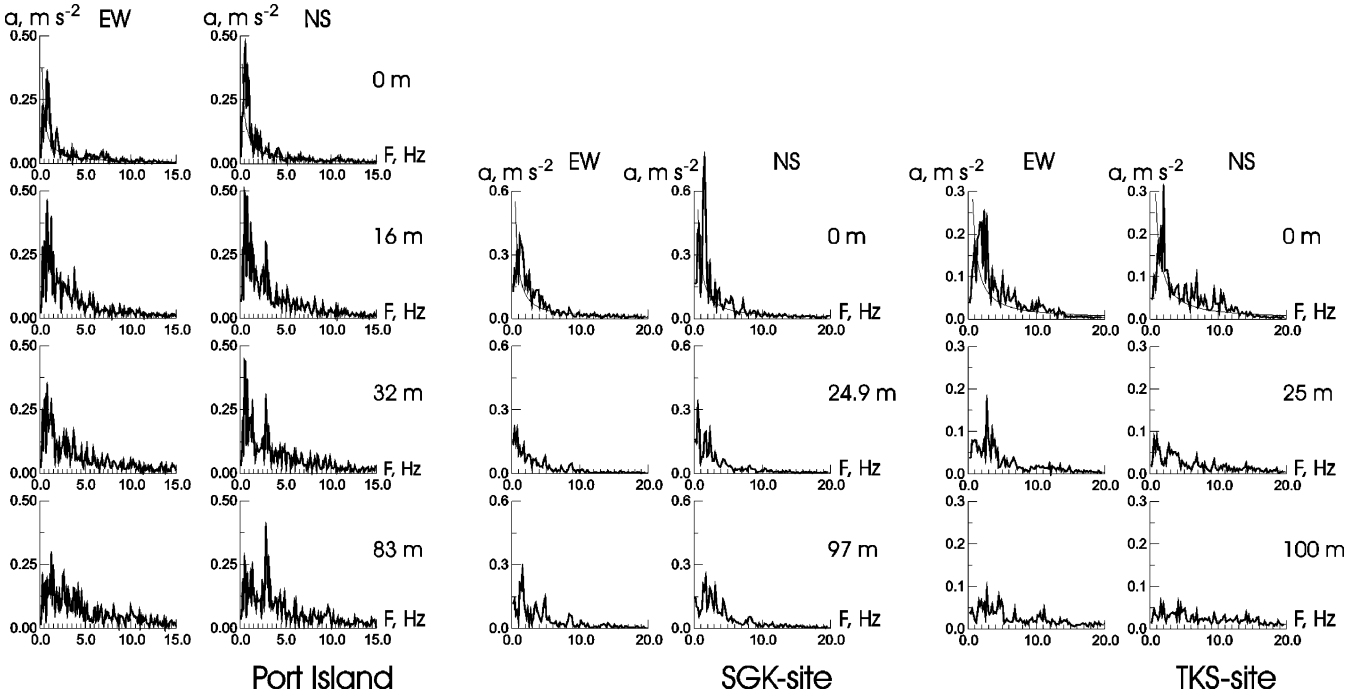

Figure 7. Acceleration spectra of the main shock of the 1995 Kobe earthquake at PI, SGK and TKS sites.

the 1995 Kobe earthquake are more close to the form $E \sim f^{-k}$ in the case of PI and less close in the case of TKS site.

Thus, intense seismic waves can suffer substantial distortions in subsurface soils; as a result, the information about the spectral composition of input signals is lost. However, the limiting shape of spectrum can be attained only in numerical simulation, when we analyse long-duration signals. In practice, we observe only the tendency of increasing low-frequency components and smoothing spectral peaks, because spectra are calculated for rather short intervals of records. Acceleration spectra of the 1995 Kobe earthquake are shown in Fig. 7 and the tendency is clearly seen: upward propagating seismic signals gain in the low-frequency components and loose sharp spectral peaks at high frequencies. As a whole, acceleration spectra of signals on the surface and at depths possess few common features.

4 CONCLUSIONS

We carried out the non-linear identification and estimated linear and non-linear components of the soil response during the 1995 Kobe earthquake at PI, SGK and TKS sites. The conclusions of the study are as follows.

The non-linear components of the soil response decreased with the distance from the fault plane from values of ∼60 per cent at PI (2 km from the fault plane) to ∼ 40 per cent at SGK (6 km from the fault plane) and to ∼13 per cent at TKS (15 km from the fault plane; the strain range is 10^{-5}–10^{-3}). Odd-order non-linear components usually predominate in the soil response, whereas even-order non-linear components become comparable to odd-order ones only in cases of liquefied soils or high intensity of the strong motion, when the loading parts of stress–strain relations in the upper layers gain noticeable even components. Constant components of seismic wavefields, i.e. quasi-static deformations of the surface, change in accord with the even-order non-linear components of the soil response. Liquefaction induces a substantial increase in the non-linear components of the soil response, from ∼40 to ∼60 per cent of the intensity of the response at PI, and changes in the predominant types of the soil non-linearity, which are the result of the rise of the even-order non-linear components of the response.

The ratio of the even-order non-linear components of the soil response during the strong motion to the odd-order non-linear components corresponds to the ratio of the even to the odd components of the loading parts of the non-linear hysteretic stress–strain relations of the upper most non-linear soil layers.

In cases of strong non-linearity, i.e. thick sedimentary layers and strong ground motion, spectra of seismic signals on the surface tend to take the form of $E \sim f^{-k}$. This limiting spectral shape was achieved at PI and SGK sites during the 1995 Kobe earthquake and $k \approx 1.2 \div 1.4$ for velocity spectra on the surface.

The proposed methods for processing vertical array records allow extracting maximum information on the soil behaviour from the records, and help in understanding the mechanisms of transformations of seismic waves in subsurface soil layers and predicting the soil behaviour during future earthquakes.

ACKNOWLEDGMENTS

We thank Yoshio Soeda, Hideki Tamai and Naoyuki Nakatsu (Kansai Electric Power Company) for acceleration records of the vertical arrays at SGK and TKS recording sites. The acceleration records of the vertical array in PI were kindly provided by Kobe City. This study was partially supported by Grant-in-Aid for Scientific Research, Nos 11792026 and 00099 Japanese Society for the promotion of Science, from the Ministry of Education, Science, Sports and Culture, Japan.

REFERENCES

Aleshin, A.S., Gushchin, V.V., Krekov, M.M., Nikolaev, A.V. & Shalashov, G.M., 1981. Experimental studies of nonlinear interaction of seismic surface waves, *Dokl. Akad. Nauk SSSR,* **260**(3), 574–575.

Archuleta, R.J., 1998. Direct observations of nonlinearity in accelerograms, in *The Effects of Surface Geology on Seismic Motion,* Vol. 1, pp. 787–792, eds Irikura, K., Okada, H. and Sasatani, T., Balkema, Rotterdam.

Archuleta, R.J. & Steidl, J.H., 2001. Borehole array data: open windows into site response. In: *10th International Conference on Soil Dynamics and Earthquake Engineering, Philadelphia, USA, October 7–10, 2001*, Volume of Extended Abstracts, vi, ed. Zerba, A., Drexel University, Philadelphia.

Bard, P.-Y. & Pitilakis, K., 1995. Seismic zonation and ground motion interface. In: *Proc. of the 5th International conference on Seismic Zonation, October. 17–19, Nice, France,* Vol. III, pp. 2127–2152, eds Pecker, A., Cluff, L., Ouest Editions, Versailles, France.

Dimitriu, P.P., 1988. Self-modulation and recurrence phenomena in vibrator-induced steady-state sinusoidal ground vibrations, *Phys. Earth planet. Int.,* **50**, 74–82.

Dimitriu, P.P., 1990. Preliminary results of vibrator-aided experiments in non-linear seismology conducted at Uetze, F.R.G., *Phys. Earth planet. Int.,* **63**, 172–180.

Field, E.H., Johnson, P.A., Beresnev, I.A. & Zeng, Y., 1997. Nonlinear ground-motion amplification by sediments during the 1994 Northridge earthquake, *Nature,* **390**, 599–602.

Groshkov, A.L. & Shalashov, G.M., 1986. Equations of nonlinear dynamics of elastic-relaxation media, *Dokl. Akad. Nauk SSSR,* **290**(4), 825–827.

Groshkov, A.L., Kalimulin, R.R. & Shalashov, G.M., 1991. Cubic nonlinear seismic effects, *Dokl. Akad. Nauk SSSR,* **315**(1), 65–68.

Gushchin, V.V. & Shalashov, G.M., 1981. On the possibility of application of nonlinear seismic effects to problems of vibro-radiation of the earth, in *Study of the Earth by nonexplosion seismic sources,* Nauka, Moscow, pp. 144–155.

Hardin, B.O. & Drnevich, V.P., 1972. Shear modulus and damping in soils: Design equations and curves, *J. Soil Mech. Found. Div.,* **98**, 667–692.

Joyner, W.B. & Chen, T.F., 1975. Calculation of nonlinear ground response in earthquakes, *Bull. seism. Soc. Am.,* **65**, 1315–1336.

Kadomtsev, B.B. & Karpman, V.I., 1871. Nonlinear waves, *Uspekhi fiz. nauk,* **103**(2), 27–48.

Kawase, H., Satoh, T., Fukutake, K. & Irikura, K., 1995. Borehole records observed at the Port Island in Kobe during the Hyogo-ken Nanbu earthquake of 1995 and its simulation, *J. Constr. Eng., AIJ,* **475**, 83–92.

Kazama, M., Yamaguchi, A. & Yanagisawa, E., 1998. Seismic behaviour of an underlying alluvial clay on man-made islands during the Hyogoken-Nanbu earthquake, *Soils and Foundations,* Special Issue, **2**, 23–32.

Korn, G.A. & Korn, T.M., 1968. *Mathematical handbook for scientists and engineers,* McGraw-Hill Book Company New York, San Francisco, Toronto, London, Sydney.

Kudo K., 1995. Practical Estimates of Site Response State-of-the-Art Report. In: *Proc. of the 5th International conference on Seismic Zonation, October 17–19, Nice, France,* Ouest Editions, Versailles, France, Vol. III, 1103–1112.

Lund, F., 1983. Interpretation of the precursor to the 1960 Great Chilean Earthquake as a seismic solitary wave, *Pageoph,* **121**(1), 17–26.

Marmarelis, P.Z. & Marmarelis, V.Z., 1978. *Analysis of Physiological Systems, The White-Noise Approach,* Plenum Press, New York and London.

O'Connell, D.R.H., 1999. Replication of apparent nonlinear seismic response with linear wave propagation models, *Science,* **283**, 2045–2050.

Pavlenko, O.V., 2001. Nonlinear Seismic Effects in Soils: Numerical Simulation and Study, *Bull. seism. Soc. Am*., **91**, 381–396.

Pavlenko, O.V. & Irikura, K., 2002. Types of elastic nonlinearity of sedimentary soils, *Geophys. Res. Lett.,* **29**(19), 36–36-4.

Pavlenko, O.V. & Irikura, K., 2003. Estimation of nonlinear time-dependent soil behaviour in strong ground motion based on vertical array data, *Pure appl. Geophys.,* accepted.

Sato, K., Kokusho, T., Matsumoto, M. & Yamada, E., 1996. Nonlinear seismic response and soil property during 1995 Hyogoken Nanbu earthquakes *Soils and Foundations*, Special issue on Geotechnical Aspects of the January 17, 1995 Hyogoken Nanbu earthquake, 41–52.

Shalashov, G.M., 1984. Cross-modulation of acoustic waves on the cubic nonlinearity in solids, *Acoustical Journal,* **XXX**(3), 386–390.

Van Den Abeele, K.E.-A. & Johnson, P.A., 1996. Elastic pulsed wave propagation in media with second- or higher-order nonlinearity. Part II. Simulation of experimental measurements on Berea sandstone, *J. acoust. Soc. Am.,* **99**, 3346–3352.

Vasil'ev, Yu.I., Ivanova, L.A. & Shcherbo, M.N., 1969. Measurement of stress and strain in a soil during the propagation of waves from explosions, *Izv. Akad. Nauk SSSR, Fiz. Zemli,* **1**, 21–37.

Zarembo, L.K. & Krasil'nikov, V.A., 1966. *Introduction to Nonlinear Acoustics,* Nauka, Moscow.

Zimenkov, S.V. & Nazarov, V.E., 1993. Nonlinear acoustic effects in rock samples, *Izv. Akad. Nauk SSSR, Fiz. Zemli,* **1**, 13–18.

Zvolinskii, N.V., 1982. Wave processes in non-elastic media, *Problems of engineering seismology,* **23**, 4–19.